Phase diagram of the two-leg Kondo ladder

J. C. Xavier and E. Miranda

Instituto de Física Gleb Wataghin, Unicamp, Caixa Postal 6165, Campinas SP 13083-970, Brazil

E. Dagotto

National High Magnetic Field Lab and Department of Physics, Florida State University, Tallahassee, Florida 32306, USA

The phase diagram of the two-leg Kondo ladder is investigated using computational techniques. Ferromagnetism is present, but only at small conduction electron densities and robust Kondo coupling J. For densities $n \gtrsim 0.4$ and any Kondo coupling, a paramagnetic phase is found. We also observed spin dimerization at densities $n = 1/4$ and $n = 1/2$. The spin-structure factor at small J peaks at $\vec{q} = (2n, 0)\pi$ for $n \lesssim 0.5$, and at $\vec{q} = (n, 1)\pi$ for $n \gtrsim 0.5$. The charge structure factor suggests that electrons behave as free particles with spin -1/2 (spin-0) for small (large) J.

Numerical studies provide valuable unbiased information about strongly correlated electronic systems. However, current computer limitations restrict most investigations to one-dimensional (1D) models or small two-dimensional (2D) clusters. Unfortunately, the physics found in 1D models is often qualitatively different from results observed in real materials. A possible procedure to start an investigation of realistic 2D models is by coupling 1D systems together. This approach has been used with great success in the case of the *t-J* model, where numerical methods, such as Exact Diagonalization[1] and Density Matrix Renormalization Group (DMRG)[2] were helpful in elucidating several properties of the 2D model through studies of *t-J* ladders.[1,3–5]

The ground-state properties of the 2D Kondo lattice model (KLM) remain mainly unexplored using unbiased methods. The KLM is the simplest model believed to describe heavy-fermion materials,[6] and, thus, a better understanding of its ground state is much needed. The main goal of the present work is to provide the first steps toward determining the phase diagram of the two-leg Kondo ladder (2-LKL). The information provided here will hopefully be as relevant for KLM 2D systems as ladder studies were in the *t-J* model context. The *N*-leg Kondo ladders consist of *N* Kondo chains coupled by the hopping term. As shown below, the phase diagram of the 2-LKL is fairly different from the 1D KLM. We considered the 2-LKL on $2 \times L$ clusters and a Hamiltonian

$$H = -t \sum_{\langle i,j\rangle,\sigma} (c_{i,\sigma}^{\dagger} c_{j,\sigma} + \text{H.c.}) + J \sum_{j} \mathbf{S}_j \cdot \mathbf{s}_j,$$

where $c_{j\sigma}$ annihilates a conduction electron at site j with spin projection σ, $\mathbf{S}_j$ is a localized spin-$\frac{1}{2}$ operator, $\mathbf{s}_j = \frac{1}{2}\sum_{\alpha\beta} c_{j,\alpha}^{\dagger} \boldsymbol{\sigma}_{\alpha\beta} c_{j,\beta}$ is the conduction electron spin-density operator, and $\boldsymbol{\sigma}_{\alpha\beta}$ are Pauli matrices. Here $\langle ij\rangle$ denotes nearest-neighbor sites, $J > 0$ is the Kondo coupling constant between conduction electrons and local moments, and $t = 1$ fixes the energy scale. The total number of conduction electrons is N and $n = N/2L$. This model was investigated with the DMRG technique[2] using open boundary conditions. The finite-size

algorithm for sizes up to $2 \times L = 80$ was applied, keeping up to $m = 1200$ states per block. The discarded weight was typically about $10^{-5} - 10^{-9}$ in the final sweep.

Let us first briefly describe what is currently known about the KLM ground-state phase diagram. In 1D, for low electronic density and/or large J, the ground state is ferromagnetic[7] (see also Ref. 8). The rest of the phase diagram is characterized by a paramagnetic phase, except for a small wedge of ferromagnetism for fillings above $n = 0.5$ (Ref. 9). Furthermore, spin dimerization has recently been discovered at $n = 0.5$ (Ref. 10). Most ground-state investigations in higher dimensions have been limited to approximate approaches. Doniach[11] pointed out the possible existence of a Kondo-lattice quantum critical point (QCP) due to the competition between the Ruderman-Kittel-Kasuya-Yosida (RKKY) interaction, which favors antiferromagnetism (AFM), and the Kondo effect, which favors paramagnetism. The full mean-field phase diagram of the 3D Kondo lattice was obtained by Lacroix and Cyrot.[12] They found that, at small J, there is a critical density n_c separating a ferromagnetic phase from an antiferromagnetic one. For sufficiently large J, however, the Kondo effect dominates and the system is paramagnetic. Further studies also considered an explicit exchange interaction between localized spins.[13] Recently, quantum Monte Carlo (QMC)[14] and DMRG[15] investigations of the half-filled Kondo lattice in small clusters confirmed the existence of a QCP at $J \sim 1.45$ in agreement with previous approximate approaches.[16] Moreover, DMRG results on *N*-leg Kondo ladders at half filling have shown that the spin and charge gaps are nonzero for any number of legs and coupling J.[15] A two-channel version has also been studied at half filling.[17] Here, the two-leg Kondo ladder *away* from half filling is considered.

In Fig. 1(a), the schematic phase diagram of the 2-LKL is presented. We have identified three phases characterized by full ferromagnetism (FM), partially saturated FM (PFM), and paramagnetism (PM). The approximate boundaries between these phases were first obtained from the energy difference $\Delta E = E((2L-N)/2) - E(0)$ for $L = 16$, where $E(p)$ is the ground-state energy in the sector with total spin projection $S_{\text{T}}^z = \sum_i S_i^z + s_i^z = p$ [Figs. 1(a) and 1(b)]. This was then refined
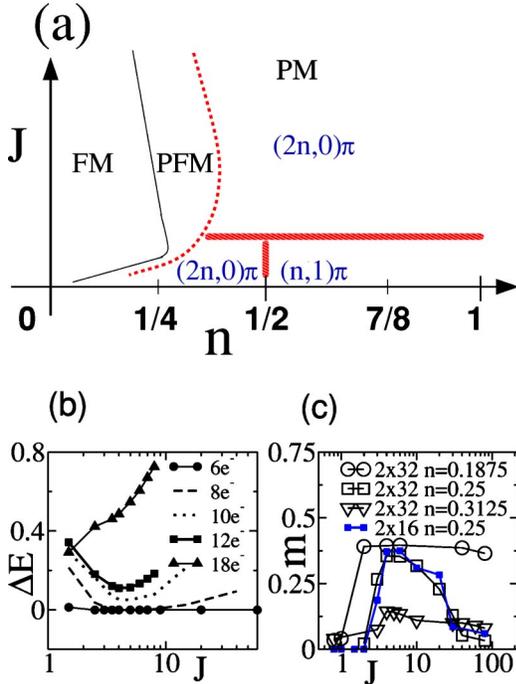
FIG. 1. (Color online) (a) Phase diagram of the 2-LKL, FM, PM, and PFM denote regions with ferromagnetism, paramagnetism, and partial ferromagnetism, respectively. To the right of the dotted line, the thick lines separate three regions: small and large J and $n \gtrsim 0.5$. These regions are characterized by the location of the spin-spin structure factor peak (see text). (b) Gap ΔE between the ground state and the ferromagnetic state vs. J for a 2×16 cluster, and several numbers of electrons (as shown). The densities from the top are, $n=0.1875$, 0.25, 0.3125, 0.374, and 0.5625. (c) Magnetization density vs. Kondo coupling, at several densities n. The errors are of the order of or smaller than the symbol size.[18]

through the (computationally more costly) calculation of the ground-state total spin in the sector $S_z=0$ of 2×8, 2×16, and 2×32 clusters [Fig. 1(c)]. In Fig. 1(b), we show ΔE as a function of J for the 2×16 cluster and several values of N.
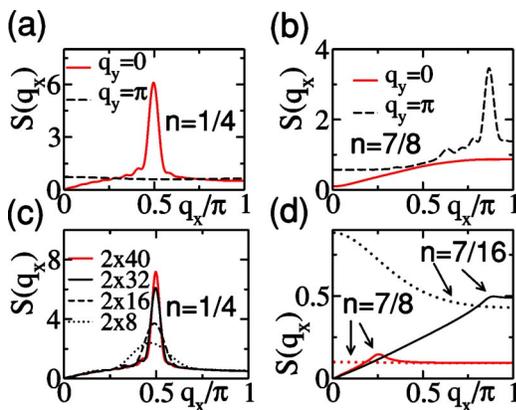
FIG. 2. (Color online) The spin structure factor $S(\vec{q})$ vs q_x for the 2-LKL: (a) $J=0.8$, $n=1/4$, and $L=32$; (b) $J=0.8$, $n=7/8$, and $L=32$; (c) $S(q_x, q_y=0)$ vs q_x for several values of L with $J=0.8$ and $n=1/4$; (d) $S(\vec{q})$ for densities $n=7/16$ and $n=7/8$ (see arrows) with $L=32$ and $J=60$. The solid (dotted) lines correspond to $q_y=0$ ($q_y=\pi$).

These values suggest that for small density and large (small) J, the ground state is FM (PM),[19] while for the whole region with density $n \gtrsim 0.4$ and $J>0$, it is PM. In Fig. 1(c), the magnetization density $m=S_T/2L$ versus J is shown for some conduction electron densities. It can be seen that for small n and J, the total spin is zero (within the DMRG precision). At $n=1/8$, m starts to increase as J is increased and saturates at $m=(1-n)/2$. For $n=1/4$, however, m is nonmonotonic and vanishes with further increase of J, apparently continuously. These results are not due to finite-size effects: the same behavior is observed for both 2×16 and 2×32 clusters at this density, suggesting that it survives the thermodynamic limit. For $0.25 \lesssim n \lesssim 0.4$, the magnetization density does not saturate at $m=(1-n)/2$ [see $n=0.3125$, Fig. 1(c)]. Then, this phase has partial ferromagnetic (PFM) order. For $n \gtrsim 0.4$, we have found that $m<0.03$ for several Kondo couplings J (while for large J, $m<10^{-3}$). This result strongly suggests that the whole region with $n \gtrsim 0.4$ is paramagnetic. This is different from the 1D KLM, which shows full FM at any
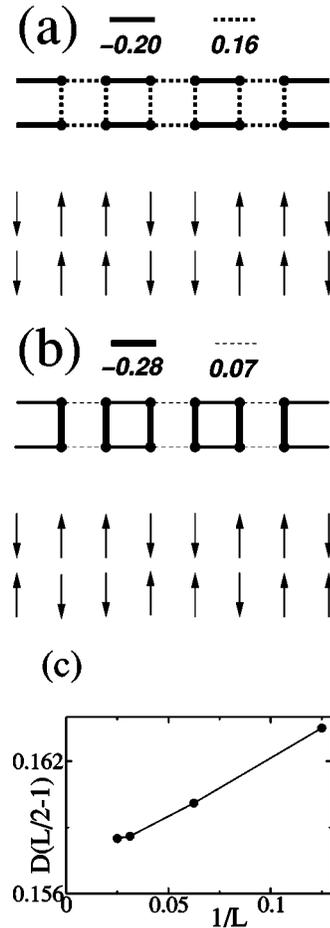
FIG. 3. (a) Nearest-neighbor spin correlations of the 2-LKL for $L=32$, $J=0.8$, and $n=1/4$. Solid and dashed lines represent AFM and FM correlations, respectively. The thickness of the lines is proportional to the magnitude of the correlations. Only the ladder central portion is presented. Below the correlations, a classical configuration compatible with them is shown. (b) Same as (a), but for $n=1/2$; (c) Dimer order-parameter $D(L/2-1)$ vs $1/L$ for $J=0.8$ and $n=1/4$.

(a)

(b)
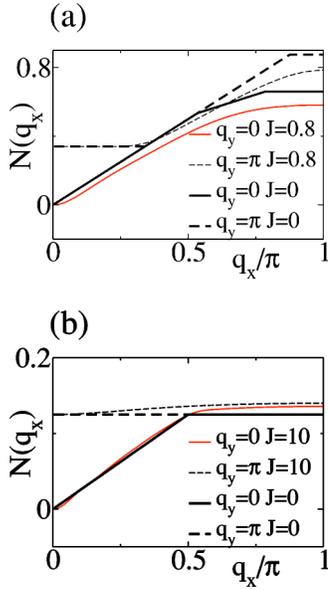
FIG. 4. (Color online) The charge structure factor $N(\vec{q})$ vs q_x for the 2×32 cluster and $n=7/8$: (a) $J=0.8$ and (b) $J=10$. We also show $N_0^{1/2}(\vec{q})$ and $N_0^0(\vec{q})$ (see text).

density for a large-enough J.[7,9] It is surprising that coupling just one more chain to the 1D Kondo lattice induces such a dramatic effect on the phase diagram.

To probe the paramagnetic phase, we calculated the Fourier transform of the spin-spin correlation function (the spin-structure factor) $S(\vec{q}) = 1/2L \sum_{\vec{r}_1, \vec{r}_2} e^{\vec{q} \cdot (\vec{r}_1 - \vec{r}_2)} \langle \mathbf{S}_{\vec{r}_1}^T \cdot \mathbf{S}_{\vec{r}_2}^T \rangle$, where $\mathbf{S}_{\vec{r}_1}^T = \mathbf{S}_{\vec{r}_1} + \mathbf{s}_{\vec{r}_1}$. We observed that the maximum of $S(\vec{q})$ can appear in three distinct positions, as indicated in Fig. 1(a). For small values of J, the maximum of $S(\vec{q})$ is located at $\vec{q} = (2n, 0)\pi$ for $n \lesssim 0.5$, while for $n \gtrsim 0.5$, it is at $\vec{q} = (n, 1)\pi$. As an example, in Figs. 2(a) and 2(b), the spin-structure factor $S(\vec{q})$ is presented for the 2×32 cluster with $J=0.8$ and densities $n=1/4$ and $n=7/8$, respectively. These results do not seem to be caused by finite-size effects, as shown in Fig. 2(c): the peak becomes more pronounced as the length L increases. Previous studies of the two-leg Hubbard model close to half filling also found that the peak of $S(\vec{q})$ appears at $\vec{q} = (n, 1)\pi$ (Ref. 4). We have also observed that, as the

density decreases from $n=1$, the peak at $\vec{q}=(n,1)\pi$ decreases, while another peak at $\vec{q}=(2n,0)\pi$ starts to increase, such that at $n \approx 0.5$ they have the same magnitude. In contrast, for large values of J, $S(\vec{q})$ is one order-of-magnitude smaller and has a small cusp at $\vec{q}=(2n,0)\pi$, as can be seen in Fig. 2(d).

Spin dimerization of the localized spins has been detected in the 1D KLM for both $J<0$[20] and $J>0$ (Ref. 10). It would be very interesting if the dimerization also survives in the 2-LKL, as this would suggest that it may also be present in the 2D system. Indeed, we have observed spin correlations in the 2-LKL that resemble the dimerization of the 1D KLM. In Fig. 3(a), we show the spin-spin correlations $\langle \mathbf{S}_{\vec{r}_1}^T \cdot \mathbf{S}_{\vec{r}_2}^T \rangle$ for nearest-neighbor sites of the 2-LKL at density $n=1/4$, $J=0.8$, and $L=32$. The solid (dashed) lines indicate that $D(j)$ is negative (positive) and the line thickness is proportional to the amplitude of the correlations. As can be seen, along the legs, the dimer order parameter $D(j) = \langle \mathbf{S}_{(1,j)}^T \cdot \mathbf{S}_{(1,j+1)}^T \rangle$ oscillates with period 2, while the rungs exhibit FM correlations. We have also found that for $n=1/2$, $D(j)$ also oscillates with period 2, as shown in Fig. 3(b). However, in this case, the correlations along the rungs are antiferromagnetic. This is not a finite-size effect artifact or caused by open boundaries. In Fig. 3(c), the order parameter at the center of the ladder $D(j=L/2-1)$ vs. $1/L$, at $J=0.8$ $n=1/4$, shows a very weak size dependence. For other densities, more complex spin structures were observed and there is no analogous simple picture (a similar situation occurs in the 1D KLM away from quarter filling[10]). For $J \gg 1$ and $0.5 \lesssim n < 1$, $\langle \mathbf{S}_{\vec{r}_1}^T \cdot \mathbf{S}_{\vec{r}_2}^T \rangle \sim -10^{-3}$ (for $n \lesssim 0.5$ some small ferromagnetic correlations start to develop), much less than the values found for small J. We also have verified that, as in the 1D case,[10] these spin correlations can be traced back to the RKKY interaction between localized spins. This effective, conduction-electron mediated spin-spin interaction can be obtained from second-order perturbation theory, and it is given by

$$H_{\mathrm{RKKY}} \sim J^2 \sum_{i,j} J_{\mathrm{RKKY}}^1(|i-j|)(\mathbf{S}_i^1 \cdot \mathbf{S}_j^1 + \mathbf{S}_i^2 \cdot \mathbf{S}_j^2)$$
$$+ 2J_{\mathrm{RKKY}}^2(|i-j|)\mathbf{S}_i^1 \cdot \mathbf{S}_j^2,$$

where

$$(J_{\mathrm{RKKY}}^1(0), J_{\mathrm{RKKY}}^1(1), J_{\mathrm{RKKY}}^1(2), \dots) = \begin{cases} (0, -1, 0.66, 0.07, -0.41, -0.03, 0.28, \dots) & n=1/4 \\ (0, -0.17, 1.25, 0.73, -1.29, 0.10, 0.46, \dots) & n=1/2 \end{cases},$$

$$(J_{\mathrm{RKKY}}^2(0), J_{\mathrm{RKKY}}^2(1), J_{\mathrm{RKKY}}^2(2), \dots) = \begin{cases} (-1.46, 0.23, 0.90, 0.09, -0.41, -0.03, 0.28, \dots) & n=1/4 \\ (4.35, 2.30, -2.42, 0.07, 0.70, 0.40, -0.86, \dots) & n=1/2 \end{cases},$$

and $\mathbf{S}_j^1$ ($\mathbf{S}_j^2$) is the localized spin in the first (second) leg and rung j. For simplicity, only the first few RKKY couplings were shown. Let us now focus on density $n=1/4$. All

$J_{\mathrm{RKKY}}^1(l)$ have signs that favor a classical configuration along the legs as $\uparrow\uparrow\downarrow\downarrow\uparrow\uparrow\downarrow\downarrow$. Note that spin dimerization is expected in a spin chain with first- and second-neighbor interactions J_1

and J_2, if $J_2 > 0$ and $-4J_2 < J_1 < 0$ (Ref. 21). The first two RKKY couplings $J^1_{RKKY}(1)$ and $J^1_{RKKY}(2)$ along the legs satisfy this inequality, and further neighbors couplings favor the classical configuration. Moreover, the couplings $J^2_{RKKY}(l)$ between legs also favor the predominant ferromagnetic alignment across the rungs (except for $J^2_{RKKY}(1) = 0.23$, which is nevertheless small), also in agreement with the classical picture presented in Fig. 3(a). A similar analysis also holds for the case $n = 1/2$. It is interesting to note that, in this case, the legs are coupled antiferromagnetically, and $J^2_{RKKY}(l)$ has larger magnitudes than at $n = 1/4$. This fact suggests that at $n = 1/2$ the legs are more strongly coupled than at $n = 1/4$. Indeed, our numerical results of Figs. 3(a) and 3(b) confirm this expectation. Thus, the RKKY interaction appears to naturally lead to the spin structure shown in Figs. 3(a) and 3(b). It is interesting to note that unusual ordered spin structures have been observed in some heavy fermion compounds (see, for example, Ref. 22). Our results suggest that the effective RKKY interaction may be their origin.

We have also calculated the charge structure factor $N(\vec{q})$ $= 1/2L \sum_{\vec{r}_1, \vec{r}_2} e^{\vec{q} \cdot (\vec{r}_1 - \vec{r}_2)} \langle \delta n(\vec{r}_1) \delta n(\vec{r}_2) \rangle$, where $\delta n(\vec{r}_1) = n(\vec{r}_1) - \langle n(\vec{r}_1) \rangle$. Previous work on the 1D KLM has shown that the qualitative behavior of $N(\vec{q})$ in the extreme weak- and strong-coupling limits could be ascribed to free spin-$\frac{1}{2}$ and spinless fermions, respectively.[23] The same analysis clarifies the behavior of $N(\vec{q})$ in the 2-LKL. Let us call $N^S_0(\vec{q})$ the charge structure factor of free fermions with spin-S in a two-leg nearest-neighbor tight-binding ladder.[23] In Fig. 4(a), $N(\vec{q})$ is shown for the 2-LKL with $L = 32$, $J = 0.8$, and $n = 7/8$, as well $N^{1/2}_0(\vec{q})$. The behavior of $N(\vec{q})$ is fairly similar to free spin-$\frac{1}{2}$ fermions. On the other hand, in the strong coupling limit $N(\vec{q})$ approaches the structure factor $N^0_0(\vec{q})$ of spinless fermions [see Fig. 4(b)].

In conclusion, we have explored the phase diagram of the two-leg Kondo lattice model away from half filling. Our results show that a ferromagnetic phase is present only for small densities, unlike the 1D Kondo chain, but consistent with mean-field studies.[12] We have found that the charges behave basically as free fermions. On the other hand, the spins have nontrivial behavior. The peak of the spin-structure factor for small values of J is located at $\vec{q} = (2n, 0)\pi$ for $n \lesssim 0.5$ and at $\vec{q} = (n, 1)\pi$ for $n \gtrsim 0.5$. For large values of J and $n \gtrsim 0.4$ $S(\vec{q})$ has only a small cusp at $\vec{q} = (2n, 0)\pi$. We have also shown that dimerization is present in the 2-LKL at densities $n = 1/4$ and $n = 1/2$, and that the RKKY interaction can tentatively explain this unusual spin arrangement.

[1] E. Dagotto, Rev. Mod. Phys. **66**, 763 (1994).

[2] S. R. White, Phys. Rev. Lett. **69**, 2863 (1992); Phys. Rev. B **48**, 10345 (1993).

[3] E. Dagotto and T. M. Rice, Science **271**, 618 (1996).

[4] R. M. Noack, S. R. White, and D. J. Scalapino, Phys. Rev. Lett. **73**, 882 (1994).

[5] S. R. White, R. M. Noack, and D. J. Scalapino, Phys. Rev. Lett. **73**, 886 (1994).

[6] A. C. Hewson, *The Kondo Problem to Heavy Fermions* (Cambridge University Press, Cambridge, England, 1993).

[7] H. Tsunetsugu, M. Sigrist, and K. Ueda, Rev. Mod. Phys. **69**, 809 (1997).

[8] G. Honner and M. Gulacsi, Phys. Rev. Lett. **78**, 2180 (1997); Phys. Rev. B **58**, 2662 (1998).

[9] I. P. McCulloch, A. Juozapavicius, A. Rosengren, and M. Gulacsi, Phys. Rev. B **65**, 052410 (2002).

[10] J. C. Xavier, R. G. Pereira, E. Miranda, and I. Affleck, Phys. Rev. Lett. **90**, 247204 (2003).

[11] S. Doniach, Physica B & C **91**, 231 (1977).

[12] C. Lacroix and M. Cyrot, Phys. Rev. B **20**, 1969 (1979).

[13] J. R. Iglesias, C. Lacroix, and B. Coqblin, Phys. Rev. B **56**, 11820 (1997); A. R. Ruppenthal, J. R. Iglesias, and M. A. Gusmão, *ibid*. **60**, 7321 (1999).

[14] F. F. Assaad, Phys. Rev. Lett. **83**, 796 (1999).

[15] J. C. Xavier, Phys. Rev. B **68**, 134422 (2003).

[16] Z. P. Shi, R. R. P. Singh, M. P. Gelfand, and Z. Wang, Phys. Rev. B **51**, 15630 (1995); Z. Wang, X. P. Li, and D. H. Lee, Physica B **199-200**, 463 (1994); K. S. D. Beach, P. A. Lee, and P. Monthoux, Phys. Rev. Lett. **92**, 026401 (2004).

[17] J. Moreno, S. Qin, P. Coleman, and L. Yu, Phys. Rev. B **64**, 085116 (2001).

[18] We defined the magnetization error as $\Delta S = |S_{m_{last}} - S_{(m_{last} - 200)}|/(S_{m_{last}} + 1)$, where S_m is the total spin of the ground state with truncation m and m_{last} is the biggest truncation available. We added 1 to the denominator so that the definition is useful also when $S = 0$.

[19] The appearance of robust FM in some regions of parameter space in both 1D and ladders should not be too surprising due to the similarities of the model with that used for manganites. See, for example, S. Yunoki *et al.*, Phys. Rev. Lett. **80**, 845 (1998).

[20] D. J. García, K. Hallberg, C. D. Batista, M. Avignon, and B. Alascio, Phys. Rev. Lett. **85**, 3720 (2000).

[21] C. Itoi and S. Qin, Phys. Rev. B **63**, 224423 (2001).

[22] E. Granado, P. G. Pagliuso, C. Giles, R. Lora-Serrano, F. Yolcaichiya, and J. L. Sarrao, Phys. Rev. B **69**, 144411 (2004).

[23] J. C. Xavier and E. Miranda, Phys. Rev. B **70**, 075110 (2004).